

Gear Fault Location Detection for Split Torque Gearbox using AE Sensors

David He¹, Pranee Manon², Ruoyu Li¹, Serap Seçkiner³, and Eric Bechhoefer⁴

¹ *Department of Mechanical & Industrial Engineering, The University of Illinois-Chicago, Chicago, IL 60607, USA*
davidhe@uic.edu
rli8@uic.edu

² *Goodrich Sensors and Integrated Systems, Vergennes, VT 05491, USA*
praneet.menon@goodrich.com

³ *Department of Industrial Engineering, University of Gaziantep, Gaziantep, Turkey*
seckiner@gantep.edu.tr

⁴ *NRG Systems, Hinesburg, VT 05461, USA*
erb@nrgsystems.com

ABSTRACT

In comparison with a traditional planetary gearbox, the split torque gearbox (STG) potentially offers lower weight, increased reliability, and improved efficiency. These benefits have driven helicopter OEMs to develop products using STG. However, the effect of multiple gears meshing simultaneously with the central gear and a large number of synchronous components (gears or bearing) in close proximity creates a problem on how to detect the gear fault location in a STG. As of today, only limited research on STG fault detection using vibration sensors and acoustic emission sensors has been conducted.

In this paper, an effective methodology on gear fault location detection using AE sensors for STG is presented. The methodology uses wavelet transform to process the AE sensor signals to determine the arrival time of the AE bursts at different locations. By analyzing the arrival times of the AE bursts, the gear fault location can be determined. The parameters of the wavelet transform are optimized by using an ant colony optimization algorithm. Real seeded gear fault experimental tests on a notational STG are conducted. AE sensor signals at the locations of healthy and damaged output driving gears are collected simultaneously to determine the location of the damaged gear. Experimental results have shown the effectiveness of the presented methodology.*

* This is an open-access article distributed under the terms of the Creative Commons Attribution 3.0 United States License,

1 INTRODUCTION

The requirement for higher energy density transmissions (lower weight) in helicopters has led to the development of the split torque gearbox (STG) to replace the traditional planetary gearbox by the drive drain designer (White, 1982). A typical split torque gearbox transmission system is shown in Figure 1. In STG, there are a number of identical gears meshing simultaneously with the central gear. This unique behavior makes the traditional vibration signal based gear fault detection algorithms, for one example, time synchronous average (TSA) ineffective in separating the interested gear fault signal. In particular, it is difficult to locate the fault inside the gearbox by analyzing the vibration signal.

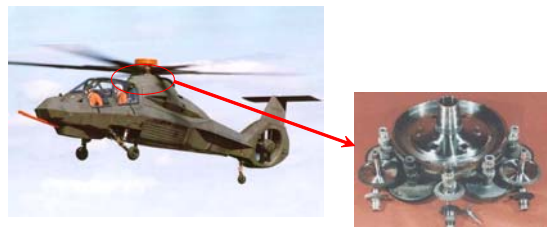


Figure 1: Comanche STG

Generally speaking, gear faults can be classified as distributed faults, such as wear, and localized faults, such as crack, chipping and so on. The distributed faults increase the transmission errors. The localized faults not only affect the transmission accuracy but also

which permits unrestricted use, distribution, and reproduction in any medium, provided the original author and source are credited.

cause catastrophic failure of the transmission system. For that reason, the research on detecting the localized faults is more important than those on detecting the distributed faults. In this paper, the gear faults refer to gear localized faults. The most commonly used techniques for gear transmission system fault detection are vibration based and acoustic emission (AE) based. The vibration signal of a gearbox carries the signature of the fault in the gears. Many signal processing methods on analyzing vibration signals to obtain the gear fault information are reported. These methods include cepstrum analysis (Dalpiaz *et al.*, 2000), TSA (McFadden, 1987; Halim *et al.*, 2008), Wigner-Ville distribution (Naim and Andrew, 2001), wavelet transform (WT) (Chen, 2002), empirical mode decomposition (EMD) (Liu *et al.*, 2006). Among these methods, time-frequency techniques, such as WT, EMD and so on are proven to be the most powerful tools on handling the non-stationary property in the vibration signal generated by the gear transmission system.

AE technique is widely used in the field of nondestructive testing (NDT). According to Eftekharijad and Mba (2009), AE is defined as the range of phenomena that result in generation of structure-borne and fluid-borne (liquid) propagating waves due to the rapid release of energy from localized sources within and /or on the surface of a material. The use of AE techniques can be found in many successful applications, such as, engine fault detection (Nivesrangan, 2005), precession manufacturing monitoring (Lee *et al.*, 2006), and wear monitoring and control (Hanchi and Klamechi, 1990). Recently, AE based approaches are beginning to attract the researchers' attention on the machine healthy monitoring. Elforjani and Mba (2009) presented a method on quantifying the crack growth in a shaft operating under slow speed. Ghamd and Mba (2006) successfully applied AE techniques to bearing fault detection. In their paper, they presented an effective methodology to determine the crack size of the bearing by measuring the width of the AE bursts. He *et al.* (2008) and Couturier and Mba (2008) showed the influence of the operational conditions on the AE based features. Eftekharijad and Mba (2009) utilized AE signals for gear fault detection. Hamzah and Mba (2009) investigated the influence of the operational conditions, such as load, rotational speed and so on, on AE based gear faults diagnosis. According to Li (2002), and Abdullah and Mba (2006), typical sources of AE waveforms generated in a rotational machinery include: (1) plastic deformation, (2) micro-fracture, (3) wear, (4) bubble, (5) friction, and (6) impacts. In comparison with vibration signals, AE signals have following advantages: (1) insensitive to structural resonances and unaffected by typical mechanical background noise, (2) more sensitive to activity from faults, (3) provides good

trending parameters. According to Elforjani and Mba (2009), normally, the frequency range of these sources is between 100 kHz and 1 MHz.

In some industrial applications, detecting fault itself is not enough. For example, in addition to locating the source of the fault in the gear transmission system, knowing which part of the system has the fault would help planning the maintenance action more effectively thus that would increase the efficiency of the maintenance and reduce the cost of the maintenance especially for those expensive parts. However, up to today, most of the research papers are concentrated on gear fault detection instead of gear fault location detection. Some papers have reported research on gear fault location detection on general gearbox. By applying TSA technique, the single gear vibration can be extracted from the vibration generated from the whole gear transmission system. Through separation, the source of the gear fault can be located. In (McFadden, 2000), the TSA was applied to identify which gear has fault. In (Blunt and Keller, 2006), TSA was utilized to separate the vibration signal for each planetary gear and sun gear of a planetary gear transmission system in the black hawk helicopters. However, in the case of STG where there are identical gears meshing simultaneously, TSA technique cannot be used effectively in separating the vibration signal of the identical gears. For AE based gear fault location detection, Toutountzakis *et al.*, (2005), attached AE sensors directly on the damaged gear for gear fault location detection. In their experiments, the sampling rates were set to be 10 MHz. In many practical applications, attaching the sensor directly on the rotational parts is impractical. Also, a sampling rate of 10 MHz will add huge burdens to both the data acquisition system and the signal processing system. Li *et al.* (2009) successfully used both AE signals and vibration signals to detect the gear faults in a notational STG. Their results showed that both AE signals and vibration signals are capable of detecting the gear faults in a STG. However, the AE signals are more sensitive to the gear fault location than the vibration signals. In their paper, the emphasis was placed on the comparison of gear fault detection performance between the AE signals and the vibration signals. No quantitative analysis of AE signals for gear fault location detection was reported in their paper.

In this paper, a methodology on gear fault location detection using AE sensors is presented. Wavelet transform is applied to process the AE signals collected from different sensor locations to determine the arrival time of the AE bursts. By analyzing the arrival time of the AE bursts, the gear fault source location can be determined. Data collected from real seeded gear fault experimental tests on a notational STG are used to

validate and demonstrate the effectiveness of the methodology.

2 GEAR FAULT LOCATION DETECTION

In concept, when traveling through a plate, the propagating waves are governed by Lamb's homogeneous equation whose solutions are called Lamb waves. Based on the general theory of wave propagation in elastic solids, AE waves propagate through a structure in a number of modes with the characteristics of dispersion and attenuation. According to Jeong and Jang (1991), if the plate is a thin one, then the velocities of the lowest symmetric (S_0) and antisymmetric (A_0) Lamb waves reduce to the plate wave solutions. To develop an AE based gear fault source location method, we can use the velocity of the waves to compute the arrival time of the waves at a limited number of sensors and hence to determine the source location. Given the nature of the AE waves, there are two possible ways to determine the arrival time. One way is to calculate the arrival time by using the information of the same part of the wave on different sensors. The other way is to calculate the arrival time by using the information of the different part of the wave on one sensor. The latter may help to reduce the number of required sensors for detection. The details of the methodology based on the first approach are provided next.

2.1 The Framework of the Methodology

Without the loss of generality and for the sake of simplicity of the demonstration, the scheme of the proposed methodology for a two-sensor system is shown in Figure 2.

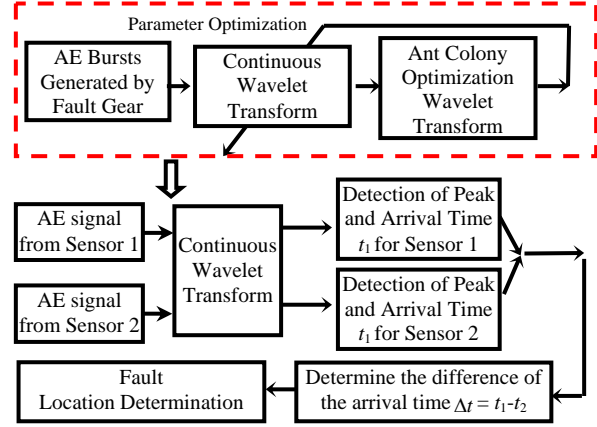


Figure 2: The scheme of the proposed methodology for a two-sensor system

As shown in Figure 2, the AE signals are first processed by continuous wavelet transform. The peak value and the arrival time t_1 , for sensor 1 and t_2 , for sensor 2, are then determined. The difference of the arrival time Δt is calculated as $t_1 - t_2$. The value of Δt could be used to determine the arrival sequence of the AE waves. If $\Delta t > 0$, it means that the AE waves reach the sensor at location 1 prior to the sensor at location 2 and vice versa. The parameters of the wavelet are optimized approximated by using ant colony optimization (ACO) method.

2.2 Theoretical Basis

2.2.1 Wavelet Transform

The wavelets can be obtained from a single function $\psi(t)$ by translation and dilation:

$$\psi(t) = \frac{1}{\sqrt{a}} \psi\left(\frac{t-\tau}{a}\right) \quad (1)$$

In Eq. (1), a is the scaling parameter, $a > 0$, τ is the time localization parameter, $\tau \in R$, and $\psi(t)$ is called the “mother wavelet”.

The wavelet transform of a finite energy signal $x(t)$ with the analyzing wavelet $\psi(t)$ is the convolution of $x(t)$ with a scaled and conjugated wavelet:

$$W(a, \tau) = \frac{1}{\sqrt{a}} \int_{-\infty}^{+\infty} x(t) \psi^*\left(\frac{t-\tau}{a}\right) dt \quad (2)$$

where $\psi^*(t)$ denotes the complex conjugate of $\psi(t)$.

In wavelet transform, the choice of a “mother wavelet” can have an impact on the processing results. Therefore, only certain types of wavelets are effective for fault diagnosis applications. Boczar and Zmarz (2004) reported that Morlet wavelet could be effective in estimating the arrival time of the AE waves.

Therefore, in this paper, a wavelet transform using Morlet wavelet is used to process the AE signals. A Morlet wavelet is defined as:

$$\psi_m(t) = \exp(-\beta^2 t^2 / 2) \exp(i\omega_0 t) \quad (3)$$

and its Fourier transform is:

$$\hat{\psi}_m(\omega) = \frac{\sqrt{\pi}}{\beta} \exp\left[-\left(\frac{\beta}{2}\right)^2 (\omega - \omega_0)^2\right] \quad (4)$$

For time-frequency analysis of dispersive waves, consider two harmonic waves of equal unit amplitude and of slightly different frequencies ω_1 and ω_2 propagating in x -direction, i.e.,

$$u(x, t) = e^{-i(k_1 x - \omega_1 t)} + e^{-i(k_2 x - \omega_2 t)} \quad (5)$$

Letting

$$k_c = (k_1 + k_2) / 2, \Delta k = (k_1 - k_2) / 2, \omega_c = (\omega_1 + \omega_2) / 2, \Delta \omega = (\omega_1 - \omega_2) / 2,$$

then Eq. (5) can be written as:

$$u(x, t) = 2 \cos(\Delta k x - \Delta \omega t) e^{-i(k_c x - \omega_c t)} \quad (6)$$

It can be seen that this resulting wave consists of two parts. The carrier wavelet represented by the exponential term propagates with phase velocity

$$c_p = \frac{\omega_c}{k_c}.$$

On the other hand, the modulated wave given by the cosine term travels with group velocity

$$c_g = \frac{d\omega}{dk}.$$

When wavelet transform is applied, the WT of $u(x, t)$ is given by (Jeong and Jang, 2000):

$$(WTu)(x, a, b) = \sqrt{a} \left\{ \begin{array}{l} e^{-i(k_1 x - \omega_1 b)} \widehat{\psi}_m(a\omega_1) \\ + e^{-i(k_2 x - \omega_2 b)} \widehat{\psi}_m(a\omega_2) \end{array} \right\} \quad (7)$$

So the magnitude of the WT is obtained as

$$|(WTu)(x, a, b)| = \sqrt{a} \sqrt{\psi_m^2(a\omega_1) + \psi_m^2(a\omega_2) + 2\psi_m(a\omega_1)\psi_m(a\omega_2)\cos(2\Delta kx - 2\Delta \omega b)} \quad (8)$$

If $\Delta \omega$ is sufficiently small such that

$$\psi^2(a\omega_1) \approx \psi^2(a\omega_2) \approx \psi^2(a\omega_c),$$

$$|(WTu)(x, a, b)| = \sqrt{2a} |\psi(a\omega_c)| \sqrt{1 + \cos(2\Delta kx - 2\Delta \omega b)} \quad (9)$$

This result indicates that the magnitude of the WT takes its maximum value at $a = \frac{\omega_0}{\omega_c}$ and

$b = \left(\frac{\Delta k}{\Delta \omega}\right)x = \frac{x}{c_g}$. In other words, the location of the peak on the (a, b) plane indicates the arrival time of the group velocity c_g at frequency $\omega_c = \frac{\omega_0}{a}$.

Though this property, we can find the arrival time of the AE bursts accurately for each location of the AE sensors. By calculating the difference of the arrival time, it is possible for us to locate the source of the gear fault.

2.2.2 Ant Colony Optimization (ACO) Algorithm

ACO is the most commonly used meta-heuristic among the methods inspired by the behavior of social insects. It has been proposed to provide a unifying framework for most combinatorial optimization problems (Stützle and Dorigo, 1999). ACO is a probabilistic technique that is designed to search and find answers to complex optimization problems in situations where the number of possible alternative solutions is vast (Seckiner and Kurt, 2008). It is widely used in solving job rotation scheduling problem (Seckiner and Kurt, 2008), Stochastic vehicle routing problem (Secomandi, 2004), Maximum independent set problem (Leguizamon *et al.*, 2001), classification problem (Martens *et al.*, 2007) and global minimization problem (Toksari, 2006). In this paper, ACO is used to search the optimal wavelet parameters with which the maximum kurtosis value of the wavelet coefficients can be achieved.

Since the kurtosis is an index of "peakness" of the signal, the objective function of the optimization is chosen to be the kurtosis of the wavelet coefficients. The kurtosis of a signal s is defined as,

$$kurt(s) = \frac{\frac{1}{N} \sum_{n=1}^N (s(n) - \bar{s})^4}{\left[\frac{1}{N} \sum_{n=1}^N (s(n) - \bar{s})^2 \right]^2} \quad (10)$$

The ACO algorithm is used to find the maximum value of the kurtosis and the flow chart of the ACO algorithm is shown in Figure 3.

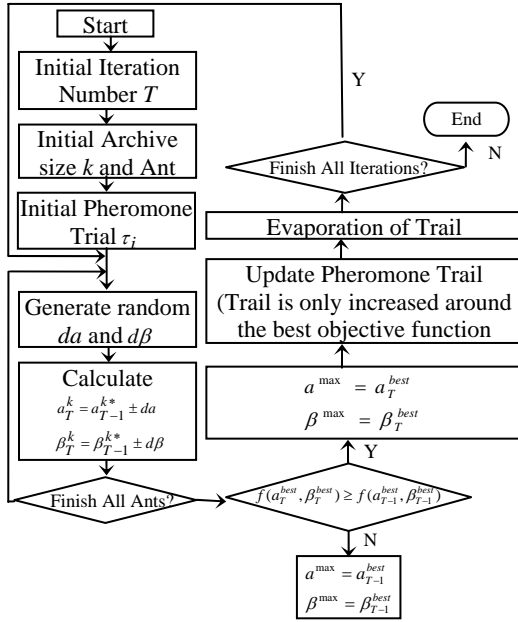


Figure 3: The flow chart of the ACO algorithm

3 EXPERIMENTAL SETUPS

In order to simulate the unique behavior of the STG, we have developed a notational STG (see Figure 4).

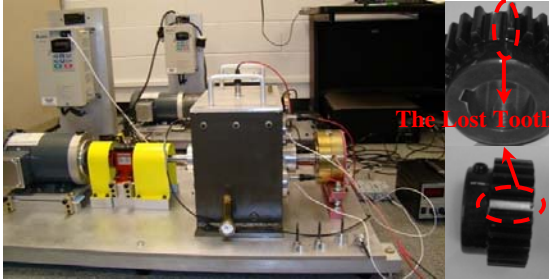


Figure 4: The notational STG

As the primary design considerations were the emulation of synchronous gear signals that would be found in a STG, for both the input side and output side of the gearbox, parallel shaft layout was used. On the input side, the input driving gear is a 40 teeth spur gear that drives three 72 teeth spur gears. On the output side, three output driving gears are 48 teeth spur gears that drive a 64 teeth spur gear. A 3-HP AC motor with a maximum speed of 3600 rpm is used to drive the notational gearbox. To accommodate for shaft misalignment and reduce the vibration transmission, a disc type coupling is utilized to transmit the torque from the motor to the driving shaft. A magnetic loading system is controlled by a power supply and the load can be adjusted by changing the output current of the amplifier. The data acquisition board is a 2-channel

data acquisition card with 18-bit resolution and the maximum sampling frequency is 40 MHz, which is 40 times of the highest response frequency of the AE sensors.

During the experiments, a WD type AE sensor was used to collect the AE signals. The operation frequency range for this type of sensor is 100 kHz to 1 MHz. In this paper, the tooth loss type seeded fault was used in the investigation. One tooth of the output driving gears was cut completely. The location of the gears on the output side of the gearbox, called output driving gear (ODG) is shown in Figure 5.

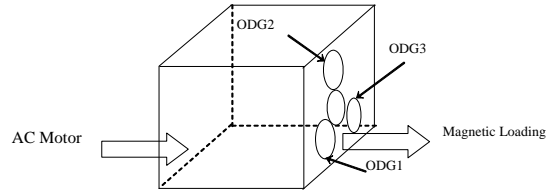


Figure 5: The location of the gears on the output side of the gearbox

4 THE RESULTS

4.1 Pencil Break Test for Sampling Rate Selection

Since a too high sampling rate may create huge burden to both the data acquisition system and signal processing system, choosing a suitable sampling rate is very important. Although the frequency range of the AE source in a rotational machine is typically between 100 kHz and 1 MHz (Elforjani and Mba, 2009), the mechanical transmission path between the AE sources and the location of the AE sensors acts as a low pass filter. Because of the effect of this low pass filter, it is necessary to conduct an experiment to determine the frequency contents of the signal picked by the AE sensors in order to choose the right sampling rate. In our experiments, a pencil lead break test was utilized to determine the sampling rate. Pencil lead break tests are widely used in the area of NDT and a pencil lead break test is a simple test that can generate a broadband AE signals. Further details on pencil lead break test can be found in (Gary and Hamstad, 1994). In our experiments, to simulate the AE bursts generated by the meshing of the damaged tooth, the pencil lead break test was conducted on the surface between the damaged output driving gear and the output driven gear.

A number of experiments were conducted using different sampling rates. Five different sampling rates were used, 50 kHz, 200 kHz, 500 kHz, 1 MHz and 2 MHz. The RMS value and the peak signal-to-noise ratio of the AE bursts under these sampling rates are provided in Table 1.

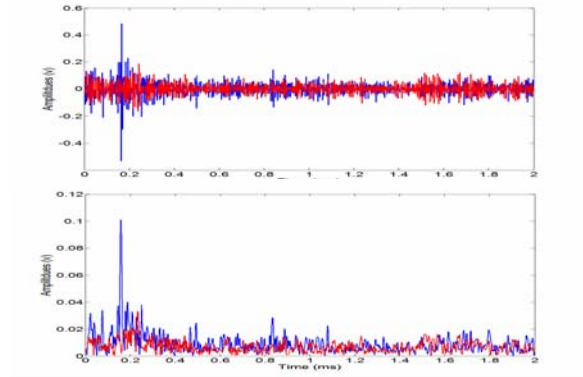
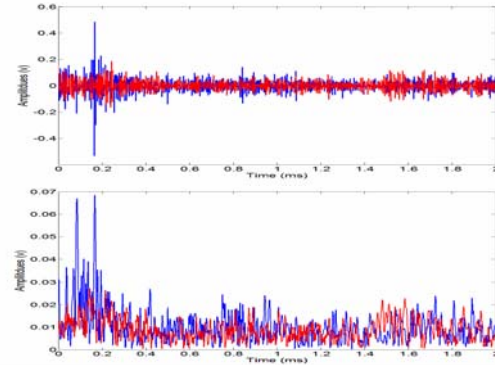
Table 1: The RMS and SNR of the AE bursts under different sampling rate

Sampling Rate	2 MHz	1 MHz	500 kHz	200 kHz	50 kHz
RMS	0.0398	0.0363	0.0318	0.0075	0.0052
Peak SNR	12.58	19.21	22.46	-	-

From Table 1, we can see that when the sampling rate is $< 500\text{kHz}$, the energy level of the AE bursts measured by RMS is reduced by one order. Therefore, the peak SNR was not calculated. This indicates that some contents in the AE bursts are lost due to the low sampling rate. However, as the sampling rate increases, the more noise contents are sampled and the SNR decreases as a result. Based on the results above, 500 kHz was selected as the sampling rate of.

4.2 Wavelet Parameters Optimization

In order to demonstrate the influence of the wavelet parameters on the wavelet coefficients, two sets of a and β values were used to process the AE bursts collected from the sensors at different locations. The results are shown in Figure 6 and Figure 7. The blue line represents the AE signals collected from the AE sensor at location 1 and the red line the AE signals collected from the AE sensor at location 2.

Figure 6: Envelope signal of the wavelet coefficient with $a=15.5$ and $\beta=1.2$ Figure 7: Envelope signal of the wavelet coefficient with $a=24$ and $\beta=2$

In Figure 6, for one set of parameter values, it is clear that we can successfully capture the arrival time of the peak of the AE bursts. However, in Figure 7, for a different set of parameter values, we cannot obtain the correct information on the arrival time of the peak of the AE bursts.

The ant colony optimization algorithm was utilized to search the optimal value of a and β . In our paper, 3 ants were used. Since for ACO the iteration number is important parameter which influences the performance of the ACO. Too small number of the iterations cannot guarantee the ACO in finding the global maximum value and too large number of the iterations will cost more time and therefore decrease the efficiency of the optimization process. In our paper, 800 iteration numbers were chosen. The parameters of the ACO were determined based on trial and error method since the main scope of this paper was not on improving the efficiency of the ACO algorithms. The time for ACO optimization is about 1.34 minutes.

In order to quantify the result obtained by ACO, the true value should be known. The kurtosis values were calculated in $a \in [1, 60]$ and $\beta \in [1, 16]$ for the step size of 0.01. The kurtosis values in the (a, β) plane is shown in Figure 8. The running time was 53 minutes, which is slower than the ACO. That means, in real-time applications, it would much quicker to use ACO to search the approximate maximum value than the exhaust search method.

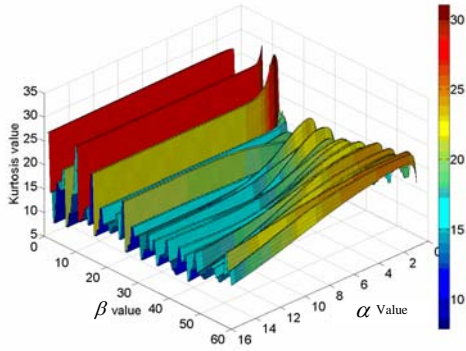


Figure 8: The Kurtosis values in the (α, β) plane

4.3 Analysis Results

Totally, 1000 AE bursts were collected for the AE sensors at two different locations. The waveforms of a sample set of AE bursts are shown in 9. The wavelet coefficients of the processed AE bursts in Figure 9 are shown in Figure 10.

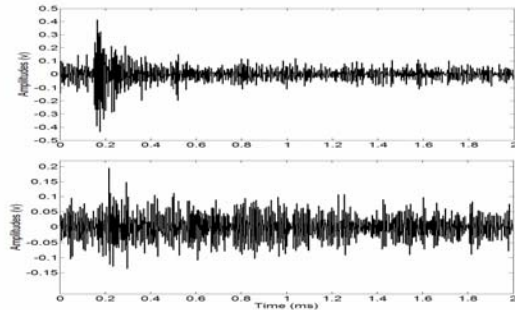


Figure 9: The AE signals: (a) at location 1 and (b) at location 2

From Figure 10, we can see that the peak amplitude at sensor location 1 occurred at 0.14 ms while the peak amplitude at sensor location 2 occurred at 0.24 ms. That is, the AE burst caused by the gear fault reached sensor 1 0.1 ms earlier than sensor 2. This is a clear indication that the gear at location 1 is a damaged one.

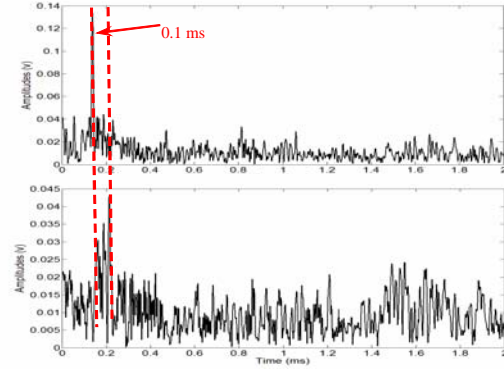


Figure 10: The processed AE signals: (a) at location 1 and (b) at location 2

Totally 1000 AE bursts for each sensor were processed in the same way and the time differences were extracted. The distribution of the time difference is shown in Figure 11. From Figure 11, we can see that the arrival time difference between 0.05 ms and 0.1 ms accounted for about 55% of all the AE bursts. And arrival time difference between 0.05 ms and 0.3 ms accounted for more than 90% of all the AE bursts. This result clearly indicates that the proposed method is effective in detecting the difference between the arrival times of the AE bursts to two different sensor locations.

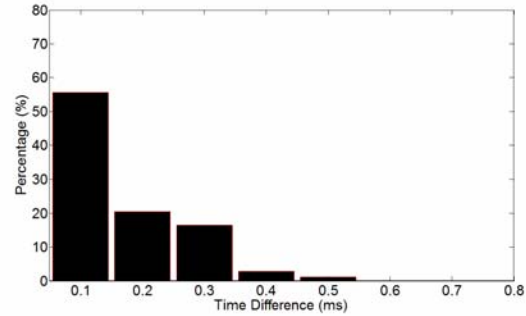


Figure 11: The distribution of the time differences between the two different locations of the sensors

5 CONCLUSION

In this paper, a methodology on STG gear fault location detection using AE sensors was presented. Wavelet transform was applied to process the AE signals collected from different sensor locations to determine the arrival time of the AE bursts. By analyzing the arrival time of the AE bursts, the gear fault source location was determined. The parameters of the wavelet were optimized by using ACO algorithm effectively. To validate the methodology and demonstrate the effectiveness of the presented method, an experimental setup using a notational STG to collect the AE signals at different locations in the gearbox was

implemented. Pencil lead break tests were first applied to determine the sampling rate of the data acquisition system. By analyzing the Fourier spectrum, RMS and peak SNR of the AE bursts from the pencil lead break tests, the sampling rate of 500 kHz was selected. AE sensor signals at the locations of healthy and damaged output driving gears were collected simultaneously to determine the location of the damaged gear. The distribution of the detected arrival times of the AE bursts coming from the damaged gear clearly indicated the effectiveness of the presented methodology.

ACKNOWLEDGMENT

The authors of the paper would like to thank Goodrich SIS for the financial support of the research project.

REFERENCES

- Abdullah M. A. and Mba D., (2006), "A Comparative Experimental Study on the Use of Acoustic Emission and Vibration Analysis for Bearing Defect Identification and Estimation of Defect Size", *Mechanical Systems and Signal Processing*, Vol. 20, pp. 1537 – 1571.
- Blunt D. M. and Keller J. A., (2006), "Detection of a Fatigue Crack in a UH-60A Planet Gear Carrier Using Vibration Analysis", *Mechanical Systems and Signal Processing*, Vol. 20, pp. 2095 – 2111.
- Boczar T. and Zmarz D., (2004), "Application of wavelet analysis to acoustic emission pulses generated by partial discharges" *IEEE Transactions on Dielectrics and Electrical Insulation*, vol. 11, p. 433.
- Chen D., (2002), "Classification of Wavelet Map Patterns using Multi-Layer Neural Networks for Gear Fault Detection", *Mechanical Systems and Signal Processing*, Vol. 16, No. 4, pp. 695 – 704.
- Couturier J. and Mba D., (2008), "Operational Bearing Parameters and Acoustic Emission Generation", *Journal of Vibration and Acoustics*, Vol. 130, No. 2, pp. 024502.1 – 024502.5.
- Dalpiaz G. Rivola A., and Rubini R., (2000), "Effectiveness and Sensitivity of Vibration Processing Techniques for Local Fault Detection in Gears", *Mechanical Systems and Signal Processing*, Vol. 14, No. 3, pp. 387 – 412.
- Eftekharijad B. and Mba D., (2009), "Seeded Fault Detection on Helical Gears with Acoustic Emission", *Applied Acoustics*, Vol. 70, pp. 547 – 555.
- Elforjani M. and Mba D., (2009), "Detecting Natural Crack Initiation and Growth in Slow Speed Shafts with the Acoustic Emission Technology", *Engineering Failure Analysis*, Vol. 16, pp. 2121 – 2129.
- Gary J. and Hamstad M., (1994), "On the far-field structure of waves generated by a pencil lead break on a thin plate", *Journal of Acoustic Emission*, vol. 12, pp. 157-170.
- Ghamd A. M. and Mba D., (2006), "A Comparative Experimental Study on the Use of Acoustic Emission and Vibration Analysis for Bearing Defect Identification and Estimation of Defect Size", *Mechanical Systems and Signal Processing*, Vol. 20, pp. 1537 – 1571.
- Halim E. B., Choudhury M. A. A. S., Shah S. L., and Zuo M. J., (2008), "Time Domain Averaging Across All Scales: A Novel Method for Detection of Gearbox Faults", *Mechanical Systems and Signal Processing*, Vol. 22, pp. 261 – 278.
- Hamzah R. I. R. and Mba D., (2009), "The Influence of Operating Condition on Acoustic Emission Generation During Meshing of Helical and Spur Gear", *Tribology International*, Vol. 42, pp. 3 – 14.
- Hanchi J. and Kiamichi B. E., (1990), "Acoustic Emission Monitoring of the Wear Process", *Wear*, Vol. 145, pp. 1 – 27.
- He Y. Y., Yin X. Y., and Chu F. L., (2008), "Modal Analysis of Rubbing Acoustic Emission for Rotor-Bearing System Based on Reassigned Wavelet Scalogram", *Journal of Vibration and Acoustics*, Vol. 130, pp. 061009.1 – 061009.8.
- Jeong H. and Jang Y. S., 2000, "Fracture Source Location in Thin Plates Using the Wavelet Transform of Dispersive Waves", *IEEE Transactions on Ultrasonics, Ferroelectrics and Frequency Control*. Vol. 47, No. 3, pp. 612 – 619.
- Lee D. E., Hwang I., Valente C. M. O., Oliveira J. F. G., and Dornfeld D. A., (2006), "Precision Manufacturing Process monitoring with Acoustic Emission", *International Journal of Machine Tools and Manufacture*, Vol. 46, No. 2, pp. 176 – 188.
- Leguizamón G., Michalewicz Z., and Schutz M., (2001), "An Ant System for the Maximum Independent Set Problem", *Proceedings of the 2001 Argentinian Congress on Computer Science*, Vol. 2, pp. 1027 – 1040.
- Li R. Y., He D., and Bechhoefer E., (2009), "Gear Fault Detection for the Split Torque Transmission System Using Acoustic Emission and Vibration Signals", *Annual Conference of the Prognostics and Health Management Society 2009*, San Diego, CA.
- Li X. L., (2002), "A Brief Review: Acoustic Emission Method for Tool Wear Monitoring During Turning", *International Journal of Machine Tools and Manufacture*, Vol. 42, pp. 157 – 165.
- Liu B., Riemenschneider S., and Xu Y., (2006), "Gearbox Fault Diagnosis Using Empirical Mode Decomposition and Hilbert Spectrum", *Mechanical*

- Systems and Signal Processing*, Vol. 20, pp. 718 – 734.
- Martens D., Backer M., Haesen R., Vanthienen J., Snoeck M., and Baesens B., (2007), “Classification with Ant Colony Optimization”, *IEEE Transactions on Evolutionary Computation*, Vol. 11, No. 5, pp. 651 – 665.
- McFadden P. D., (2000), “Detection of Gear Faults by Decomposition of Matched Differences of Vibration Signals”, *Mechanical Systems and Signal Processing*, Vol. 14, No. 5, pp. 805 – 817.
- McFadden. P. D., (1987), “A Revised Model for the Extraction of Periodic Waveforms by Time Domain Averaging”, *Mechanical Systems and Signal Processing*, Vol. 1, No. 1, pp. 83 – 95.
- Naim B. and Andrew B., (2001), “A Comparative Study of Acoustic and Vibration Signals in Detection of Gear Failures Using Wigner-Ville Distribution”, *Mechanical Systems and Signal Processing*, Vol. 15, No. 6, pp. 1091 – 1107.
- Nivesrangan P., Steel J. A., and Reuben R. L., (2005), “AE Mapping of Engines for Spatially Located Time Series”, *Mechanical Systems and Signal Processing*, Vol. 21, No. 2, pp. 1084 – 1102.
- Seckiner S.U. and Kurt M., (2008), “Ant Colony Optimization for the Job Rotation Scheduling Problem”, *Applied Mathematics and Computation*, Vol. 201, pp. 149 -160.
- Secomandi N., (2004), “Comparing Neuro-Dynamic Programming Algorithms for the Vehicle Routing Problem with Stochastic Demands”, *Computers & Operation Research*, Vol. 27, No. 11, pp. 1201 – 1225.
- Stützle, T. and Dorigo, M. (1999) “ACO algorithms for the traveling salesman problem”, in K. Miettinen, M. Makela, P. Neittaanmaki and J. Periaux (Eds.) *Evolutionary Algorithms in Engineering and Computer Science: Recent Advances in Genetic Algorithms, Evolution Strategies, Evolutionary Programming, Genetic Programming and Industrial Applications*, John Wiley & Sons.
- Toksari M. D., (2006) “Ant Colony optimization for finding the global minimum”, *Applied Mathematics and Computation*, Vol. 176, pp. 308-316.
- Toutountzakis T., Tan C. K., and Mba D., (2005), “Application of Acoustic Emission to Seeded Gear Fault Detection”, *NDT&E International*, Vol. 38, pp. 27 -36.
- White G., (1982), “Split Torque Transmission”, *USPTO*, 4,489,625, 1982.